

ROAST: an open-source, fully-automated, Realistic vOlumetric-Approach-based Simulator for TES*

Yu Huang^{1,2}, Abhishek Datta², Marom Bikson¹ and Lucas C. Parra¹

Abstract—Research in the area of transcranial electrical stimulation (TES) often relies on computational models of current flow in the brain. Models are built on magnetic resonance images (MRI) of the human head to capture detailed individual anatomy. To simulate current flow, MRIs have to be segmented, virtual electrodes have to be placed on the scalp, the volume is tessellated into a mesh, and the finite element model is solved numerically to estimate the current flow. Various software tools are available for each step, as well as processing pipelines that connect these tools for automated or semi-automated processing. The goal of the present tool – ROAST – is to provide an end-to-end pipeline that can automatically process individual heads with realistic volumetric anatomy leveraging open-source software (SPM8, iso2mesh and getDP) and custom scripts to improve segmentation and execute electrode placement. When we compare the results on a standard head with other major commercial software for finite element modeling (ScanIP, Abaqus), ROAST only leads to a small difference of 9% in the estimated electric field in the brain. We obtain a larger difference of 47% when comparing results with SimNIBS, an automated pipeline that is based on surface segmentation of the head. We release ROAST as an open-source, fully-automated pipeline at <https://www.parralab.org/roast/>.

I. INTRODUCTION

Research in transcranial electrical stimulation (TES) heavily relies on computational models of the current flow in the brain, which are built based on individual head anatomy as captured with magnetic resonance imaging (MRI) [1], [2]. The major steps for this modeling process include segmenting the MRI into different tissue compartments, assigning conductivity to each tissue, placing virtual electrodes on the models, tessellating this volumetric anatomy into a 3D mesh, and numerically solving for the voltage distribution on this finite element model (FEM) [1]. Various software tools are available for each step. For example, SPM (Statistical Parametric Mapping, [3]), FSL (FMRIB Software Library [4]) and FreeSurfer [5] can all generate segmentations for the brain and head, with each one having different pros and cons (see [6] for a complete review). Generation of an FEM can be accomplished by either open-source tools (e.g. iso2mesh [7], Gmsh [8]) or proprietary software (e.g. ScanIP (Simpleware Ltd, Exeter, UK), Mimics (Materialise NV, Leuven, Belgium)). The same is true for FEM solvers (open-source: getFEM++ [9], getDP [10]; commercial: Abaqus (SIMULIA,

Providence, RI), COMSOL Multiphysics (COMSOL Inc., Burlington, MA)).

Given this great variety and complexity, there is a need to automate these tools into a complete processing pipeline. Existing pipelines are either not fully automated (e.g. NFT [11]) or difficult to use (e.g. SciRun [12]). Notable in terms of ease of use (if not of installation) is SimNIBS [13], which integrates FreeSurfer, FSL, Gmsh and getDP to provide a complete end-to-end solution, based on the surface segmentation of the head. In the TES modeling literature, however, FEM based on volumetric segmentation is preferred over boundary element method (BEM) that is more common for EEG modeling, e.g. [14]. While it can capture the detailed gyral/sulcal surfaces, BEM has limited abilities to represent the anatomical morphology. For instance, boundary surfaces between tissues need to be entirely contained within one another, making it difficult to implement anatomical details such as the optic foramen. Moreover, it is more computationally expensive to generate the surface segmentation for BEM [5] compared to volumetric segmentation algorithm based on probability inferences [15], which is the major reason why SimNIBS needs ~ 10 hours to run segmentation. We aimed to generate a fast automated pipeline that operates entirely with volumes and does not have the morphological restrictions imposed by surface segmentation.

To this end we use the segmentation algorithm in SPM8 and apply it to the entire head and neck [16]. We integrate this with our tools to ensure continuity of the cerebrospinal fluid (CSF) and skull and to automatically place electrodes. This is followed by meshing with iso2mesh and FEM solving with getDP. Finally, we use volumetric visualization of the resulting electric fields (Figure 1). The complete pipeline is a Realistic vOlumetric Approach to Simulate Transcranial Electric Stimulation (ROAST). ROAST is based on Matlab but is otherwise entirely open source. It processes individual MRI volumes in a fully automated fashion to generate 3D renderings of the resulting current distributions. The user can specify any number of electrodes within the 10-05 system. The end-to-end processing time is typically less than 30 minutes, which is one order of magnitude faster than alternative approaches (e.g. SimNIBS). It is also significantly easier to use as compared to other tools (e.g. SCIRun).

Results of ROAST on the MNI-152 standard head [17] are compared here to SimNIBS and results obtained with a commercial mesher and solver (ScanIP and Abaqus). To our knowledge this is the first comparative evaluation of these TES modeling tools. Results show that ROAST only deviates 9% in predicting the electric fields in the brain. The differ-

*This work was supported by the NIH through grants R01MH11896, R44NS092144, R41NS076123, and by Soterix Medical Inc.

¹Y. Huang, M. Bikson and L.C. Parra are with the Department of Biomedical Engineering, City College of the City University of New York, New York, NY 10031, USA yhuang16@citymail.cuny.edu

²Y. Huang and A. Datta are with Research & Development, Soterix Medical, Inc., New York, NY 10001, USA yhuang@soterixmedical.com

ence is higher (47%) when comparing the output of ROAST with that of SimNIBS. We release ROAST now at <https://www.parralab.org/roast/> to make current-flow models accessible to a broader group of researchers.

II. METHODS

Starting from a standard head (MNI-152 v6, [17]), we tested and compared the results for five different modeling workflows for TES with electrodes at locations Fp2 and Iz. Figure 1 shows these five candidates. The red and blue outlines highlight ROAST and SimNIBS, respectively, and the circled numbers on the right indicate each pipeline.

For Pipelines 1–4, the MNI-152 MRI was segmented using SPM8 (the New Segment routine [15], [16]). Automatic touch-up on the segmentation results were performed by morphological operations [16]. This conservative post-processing attempts to, but does not fully, remove holes on gray matter, CSF and skull. Remaining holes were filled using simple heuristics (e.g., to fill holes on CSF, check if any brain voxel touches bone/skin/air, if so, then convert the bone/skin/air neighbor to CSF). This heuristics is applied to all the holes in gray matter and CSF, but selectively to skull, as we want to preserve certain skull openings (e.g., the optic canal and foramen magnum). To this end, a special mask was made marking up these regions in the prior tissue probability maps used by the New Segment and this mask was mapped into the individual MRI space during segmentation. These regions were then treated as exceptions during the patching process. Electrodes (Fp2, Iz) were then placed on the scalp surface using Matlab scripts developed in [16]. In Pipeline 1, the “cgalv2m” function was used in iso2mesh [7] to generate a volumetric mesh directly from segmented MRI. This is made possible by the CGAL package [18], which is capable of generating a volumetric mesh from 3D multi-domain images. A customized Matlab function was written to set up the boundary conditions with 1 A/m² current density applied on Fp2, and call the solver getDP [10] to solve the underlying Laplacian equation [19]. The same conductivity values are used as in [16]. In Pipeline 2, adaptive meshing (ScanFE-Free algorithm) was used in ScanIP and the output mesh was converted to .msh format for solving in getDP. Pipeline 3 essentially follows the same details as in [16]. In Pipeline 5, the MNI-152 head was segmented by the combination of FSL and FreeSurfer (part of SimNIBS [13]). Electrode placement was done in SimNIBS graphic user interface (GUI) by entering the exact coordinates on the scalp surface (obtained from Pipeline 1). The model was then solved in SimNIBS by clicking the “Run” button in the GUI. To compare how SimNIBS-generated segmentation affects the modeling results compared to SPM8-generated segmentation, we feed the segmented masks from SPM8 into gmsh and getDP, leading to Pipeline 4. Since gmsh only accepts surface segmentation as its input format [8], the volumetric masks from SPM8 were first converted into .stl format using iso2mesh in Pipeline 4 before entering gmsh.

The solutions on the mesh node were read into Matlab and interpolated onto a regular grid with the same dimensions and

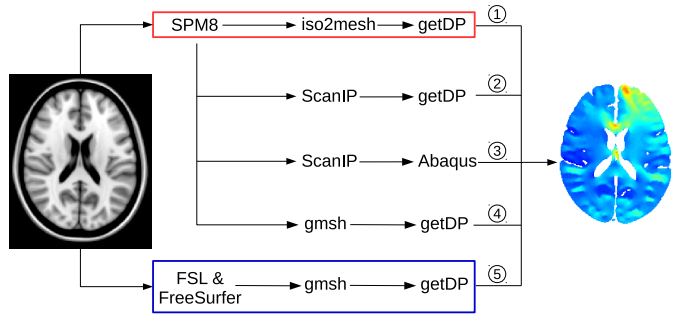


Fig. 1. Candidate pipelines for building a current-flow model of the head. The input and output of each pipeline is the MRI and the electric field distribution, respectively.

resolution as the original MRI. Voxel-to-voxel comparison on the electric field distribution can then be performed across the methods. Furthermore, model predictions from Pipelines 1–4 were all calibrated to correspond to 1 mA current injection at the anode Fp2, by using the exact anode area calculated from the tetrahedral mesh elements. For Pipeline 5, the injected current was also set to 1 mA at Fp2 in the SimNIBS GUI. The metric to quantify the difference between two methods A and B is the deviation of A from B, with B as the reference (i.e., the relative difference):

$$d = \frac{\|\mathbf{E}_A - \mathbf{E}_B\|}{\|\mathbf{E}_B\|} \times 100\%. \quad (1)$$

Here \mathbf{E} indicates the electric field. We compare the results of the open-source tools to the commercial FEM software and the results using the SPM8 segmentation to the SimNIBS segmentation. Segmentation masks were used to extract the tissue-specific electric field. For Pipelines 1–4, SPM8-generated segmentations were used. For Pipeline 5, since SimNIBS generates embedded structures separately (see Section III for details), these tissue masks were first manually processed to be consistent with SPM8’s masks, e.g., merging ventricles into CSF. The resulting five tissue masks (gray matter, white matter, CSF, skull, and scalp) were used to extract the electric field. Air cavities inside the skull are not provided by SimNIBS, instead, they are labeled as skull.

For Pipeline 1, we put all needed open-source tools and customized scripts into one single package named ROAST and made it available online at <https://www.parralab.org/roast/>. As a fully-automated pipeline, users do not have to install separate packages. They only need to install Matlab, download ROAST, and enter a one-line command that selects the desired MRI (in NIfTI format) and the desired electrode locations (in 10-05 system nomenclature) with the amount of injected current. A simulation result will then be generated within 15–30 minutes (tested on a typical dual-core computer with 8 GB memory).

III. RESULTS

Figure 2 shows an axial brain slice of the electric field distribution from the five modeling methods in Figure 1, with the corresponding histograms of the field magnitude

in the brain. It is evident that the relative distributions of electric fields in the brain are visually quite similar across different modeling pipelines, except for results from SimNIBS, which has more detailed sulcal structures due to the surface approach for segmentation in FreeSurfer. The overall magnitude distribution of fields is also remarkably similar (histograms on the right column). The quantitative differences for the electric field distributions as calculated from Eq. 1 between these methods are shown in Figure 3, where we essentially compared five pairs of pipelines, as indicated by the five columns. The title at each column indicates which two pipelines were compared. Comparing Pipeline 1 vs. 2 shows the difference introduced from using open-source mesher iso2mesh instead of the commercial ScanIP (Figure 3A); Pipeline 2 vs. 3 gives the difference between the free solver getDP (Figure 3B) and commercial solver Abaqus; Pipeline 1 vs. 3 captures the difference between iso2mesh/getDP and ScanIP/Abaqus (Figure 3C); Pipeline 4 vs. 2 gives the difference between gmsh and ScanIP (Figure 3D); Pipeline 5 vs. 4 shows the difference between the segmentation generated by SimNIBS vs. ROAST (Figure 3E).

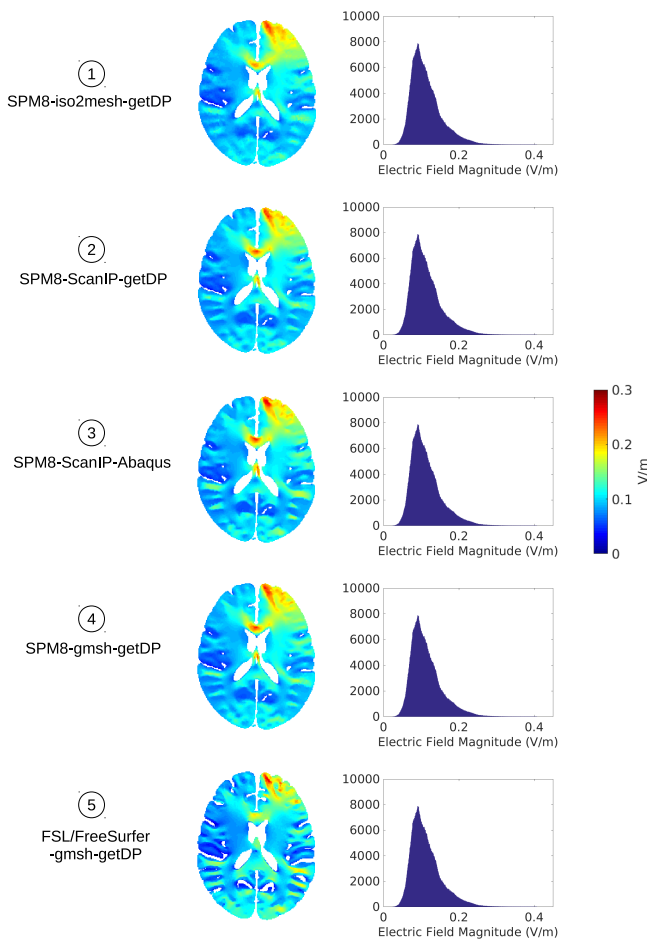


Fig. 2. Example brain slices showing electric field distributions output by the five modeling methods from Figure 1.

Relative differences in electric fields from using open

source versus commercial meshers and solvers are an average of 20% (Figure 3A–D), with differences in the CSF shooting up over 100% when getDP is used instead of Abaqus (Figure 3B). This is expected as the CSF is a very thin layer with a high jump of conductivity from its neighboring tissues. Different solvers handle this discontinuity differently when computing the electric field from the solved voltages [20]. SimNIBS-generated segmentation gives higher deviations (average 67%, Figure 3E) in electric field compared to those from SPM8-generated segmentation. This indicates the genuine difference in these two categories of modeling methods (i.e., Pipeline 1–4 vs. Pipeline 5). The source of this difference comes mainly from the two different segmentation approaches. While SPM8 segmentation algorithm works on voxelized image data [15], SimNIBS, which utilizes FSL [4] and FreeSurfer [5], generates the segmentation in the format of a surface mesh. This can give great details of the gyri and sulci on the cortex, even when tested on the MNI-152 head which is an averaged anatomy. On the other hand, SPM-generated brain segmentation does not include these details. However, one limitation of the surface-based segmentation is that each tissue volume is defined as the space between two surfaces (e.g., skull volume is between scalp and skull surface). Therefore, embedded structures (e.g., ventricles inside surface CSF), components with intersecting surfaces (e.g., gray matter and cerebellum), and tissues with disconnected regions (e.g., skull with floating structures of spine) cannot be defined from a single, self-closed, non-intersecting surface, unless each structure is defined separately. Future work may consider combining the brain segmentation from FreeSurfer with the skull/scalp segmentation from SPM for building improved TES models.

IV. CONCLUSIONS

This paper proposes a new pipeline for TES modeling, which we have termed ROAST. It is a fully automated simulator based on free software (but does leverage Matlab to reuse several existing tools). Using the volumetric segmentation from SPM, it allows for a more realistic modeling of the anatomy and runs faster (15–30 minutes) compared to SimNIBS (10 hours). Also, as the dependent libraries are included in a single package (for Linux, Windows, and Mac), it is easy and straightforward to use, without the need to install software (other than Matlab). It only gives a 9% difference in predicted electric field distribution when compared to commercial FEM software.

Finally, we want to emphasize that all the differences reported in this paper are not indicative of better or worse performance relative to the true current flows in the brain. Future work is needed to validate which modeling method gives more accurate predictions. On a very basic level we intend to validate meshing and solving by comparing to analytic solutions of a spherical model [21] for which we provided a software interface (<https://www.parralab.org/spheres/>). To validate the performance of anatomical segmentation for the purpose of current-flow modeling, one can use *in vivo* intracranial recordings in humans [22], which

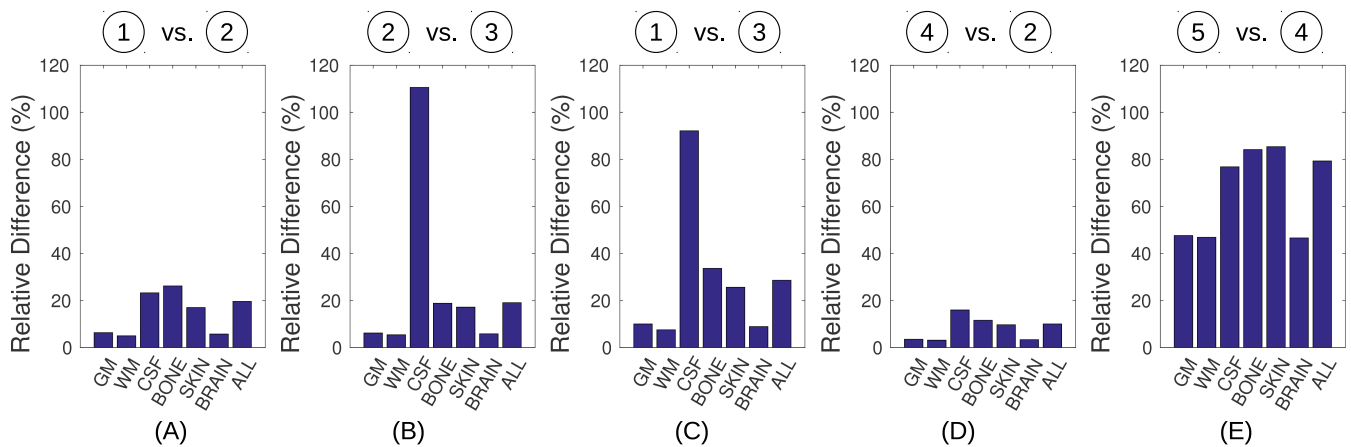


Fig. 3. Comparisons between different pipelines in terms of how they predict the electric field distributions. Each bar represents the relative difference for the corresponding tissue as computed from Eq. 1. GM: gray matter; WM: white matter; CSF: cerebrospinal fluid; BRAIN: gray and white matter; ALL: all the tissues combined.

we have already made publicly available (<https://www.parralab.org/tesValidate/>).

ACKNOWLEDGMENT

The authors would like to thank Chris Thomas at Soterix for insightful discussions. We also would like to thank Alexander Opitz for pointing us to the free solver getDP. We also thank Jens Madsen for assistance with Matlab GUI programming. This work was supported by the NIH through grants R01MH111896, R44NS092144, R41NS076123, and by Soterix Medical Inc.

REFERENCES

- [1] A. Datta, V. Bansal, J. Diaz, J. Patel, D. Reato, and M. Bikson, "Gyri-precise head model of transcranial DC stimulation: Improved spatial focality using a ring electrode versus conventional rectangular pad," *Brain stimulation*, vol. 2, no. 4, pp. 201–207, Oct. 2009.
- [2] P. Luu, E. M. Essaki Arumugam, E. Anderson, A. Gunn, D. Rech, S. Turovets, and D. M. Tucker, "Slow-Frequency Pulsed Transcranial Electrical Stimulation for Modulation of Cortical Plasticity Based on Reciprocity Targeting with Precision Electrical Head Modeling," *Frontiers in Human Neuroscience*, vol. 10, p. 377, 2016.
- [3] K. J. Friston, *Statistical Parametric Mapping: The analysis of functional brain images*. Amsterdam: Elsevier/Academic Press, 2007.
- [4] S. M. Smith, M. Jenkinson, M. W. Woolrich, C. F. Beckmann, T. E. J. Behrens, H. Johansen-Berg, P. R. Bannister, M. De Luca, I. Drobnjak, D. E. Flitney, R. K. Niazy, J. Saunders, J. Vickers, Y. Zhang, N. De Stefano, J. M. Brady, and P. M. Matthews, "Advances in functional and structural MR image analysis and implementation as FSL," *NeuroImage*, vol. 23 Suppl 1, pp. S208–219, 2004.
- [5] A. M. Dale, B. Fischl, and M. I. Sereno, "Cortical surface-based analysis. I: segmentation and surface reconstruction," *NeuroImage*, vol. 9, no. 2, pp. 179–194, Feb. 1999.
- [6] Y. Huang and L. C. Parra, "Fully Automated Whole-Head Segmentation with Improved Smoothness and Continuity, with Theory Reviewed," *PLOS ONE*, vol. 10, no. 5, p. e0125477, May 2015.
- [7] Q. Fang and D. Boas, "Tetrahedral mesh generation from volumetric binary and grayscale images," in *IEEE International Symposium on Biomedical Imaging: From Nano to Macro, 2009. ISBI '09*, Jul. 2009, pp. 1142–1145.
- [8] C. Geuzaine and J.-F. Remacle, "Gmsh: A 3-D finite element mesh generator with built-in pre- and post-processing facilities," *International Journal for Numerical Methods in Engineering*, vol. 79, no. 11, pp. 1309–1331, 2009.
- [9] Y. Renard and J. Pommier, "GETFEM: A generic finite element library in C," 2010, <http://download.gna.org/getfem/html/homepage/index.html>.
- [10] P. Dular, C. Geuzaine, F. Henrotte, and W. Legros, "A general environment for the treatment of discrete problems and its application to the finite element method," *IEEE Transactions on Magnetics*, vol. 34, no. 5, pp. 3395–3398, Sep. 1998.
- [11] Z. A. Acar and S. Makeig, "Neuroelectromagnetic forward head modeling toolbox," *Journal of Neuroscience Methods*, vol. 190, no. 2, pp. 258–270, Jul. 2010.
- [12] M. Dannhauer, D. Brooks, D. Tucker, and R. MacLeod, "A pipeline for the simulation of transcranial direct current stimulation for realistic human head models using SCIRun/BioMesh3D," in *2012 Annual International Conference of the IEEE Engineering in Medicine and Biological Society (EMBC)*, Sep. 2012, pp. 5486–5489.
- [13] M. Windhoff, A. Opitz, and A. Thielscher, "Electric field calculations in brain stimulation based on finite elements: An optimized processing pipeline for the generation and usage of accurate individual head models," *Human Brain Mapping*, vol. 34, no. 4, pp. 923–935, 2011.
- [14] M. Fuchs, R. Drenckhahn, H. Wischmann, and M. Wagner, "An improved boundary element method for realistic volume-conductor modeling," *IEEE Transactions on Biomedical Engineering*, vol. 45, no. 8, pp. 980–997, 1998.
- [15] J. Ashburner and K. J. Friston, "Unified segmentation," *NeuroImage*, vol. 26, no. 3, pp. 839–851, Jul. 2005.
- [16] Y. Huang, J. P. Dmochowski, Y. Su, A. Datta, C. Rorden, and L. C. Parra, "Automated MRI segmentation for individualized modeling of current flow in the human head," *Journal of Neural Engineering*, vol. 10, no. 6, p. 066004, Dec. 2013.
- [17] G. Grabner, A. L. Janke, M. M. Budge, D. Smith, J. Pruessner, and D. L. Collins, "Symmetric atlas and model based segmentation: an application to the hippocampus in older adults," *Medical image computing and computer-assisted intervention: MICCAI: International Conference on Medical Image Computing and Computer-Assisted Intervention*, vol. 9, no. Pt 2, pp. 58–66, 2006.
- [18] L. Rineau, S. Tayeb, and M. Yvinec, "3D mesh generation," in *CGAL User and Reference Manual*, 3rd ed., CGAL Editorial Board, Ed., 2009. [Online]. Available: http://www.cgal.org/Manual/3.5/doc.html/cgal_manual/packages.html#Pkg:Mesh.3
- [19] D. J. Griffiths, *Introduction to electrodynamics*, 3rd ed. Upper Saddle River, NJ: Prentice Hall, 1999.
- [20] C. Engwer, J. Vorwerk, J. Ludewig, and C. H. Wolters, "A discontinuous galerkin method to solve the eeg forward problem using the subtraction approach," *SIAM Journal on Scientific Computing*, vol. 39, no. 1, pp. B138–B164, 2017.
- [21] J. P. Dmochowski, M. Bikson, and L. C. Parra, "The point spread function of the human head and its implications for transcranial current stimulation," *Physics in medicine and biology*, vol. 57, no. 20, pp. 6459–6477, Oct. 2012.
- [22] Y. Huang, A. A. Liu, B. Lafon, D. Friedman, M. Dayan, X. Wang, M. Bikson, W. K. Doyle, O. Devinsky, and L. C. Parra, "Measurements and models of electric fields in the in vivo human brain during transcranial electric stimulation," *eLife*, vol. 6, p. e18834, Feb. 2017.